NUCL SCI TECH (2020) 31:55
https://doi.org/10.1007/s41365-020-00762-1

Study on cosmogenic radioactive production in germanium as a background for future rare event search experiments

Yu-Lu Yan[1] · Wei-Xin Zhong[2] · Shin-Ted Lin[1] · Jing-Jun Zhu[3] · Chen-Kai Qiao[1] · Lei Zhang[1] · Yu Liu[1] · Qian Yue[4] · Hao-Yang Xing[1] · Shu-Kui Liu[1]

Received: 25 December 2019 / Revised: 8 March 2020 / Accepted: 29 March 2020 / Published online: 19 May 2020

Abstract Rare event search experiments are one of the most important topics in the field of fundamental physics, and high-purity germanium (HPGe) detectors with an ultra-low radioactive background are frequently used for such experiments. However, cosmogenic activation contaminates germanium crystals during transport and storage. In this study, we investigated the movable shielding containers of HPGe crystals using Geant4 and CRY Monte Carlo simulations. The production rates of ^{68}Ge, ^{65}Zn, ^{60}Co, ^{55}Fe, and ^{3}H were obtained individually for different types of cosmic rays. The validity of the simulation was confirmed through a comparison with the available experimental data. Based on this simulation, we found that the interactions induced by neutrons contribute to approximately 90% of the production rate of cosmogenic activation. In addition, by adding an optimized shielding structure, the production rates of cosmogenic radionuclides are reduced by about one order of magnitude. Our results show that it is feasible to use a shielding container to reduce the cosmogenic radioactivity produced during the transport and storage of high-purity germanium on the ground.

Keywords High-purity germanium · Shielding structure · Geant4 · Transportation

1 Introduction

Rare event experiments, such as the search for neutrinoless double beta decay ($0\nu\beta\beta$) [1–3] and the direct detection of weakly interacting massive particles (WIMPs) [4, 5], are critical fundamental topics for understanding physics beyond the standard model. Observations of neutrinoless double beta decay will help researchers study whether neutrinos are Majorana or Dirac particles and establish physics beyond the standard model when the lepton number is not conserved [6, 7].The direct detection of WIMPs will help us answer many important open questions in physics and provide a better understanding of the universe and its evolution [8]. Both types of experiments involve searching for extremely rare signals. Thus, high-mass and high-sensitivity detectors with an ultra-low background environment are required. Experiments including EDELWEISS-III [9] have shown that the envisioned background level is $\sim$ 1 count/kg/keV/day (cpkkd) at 2–3 keVee. CDMSLite [10] can achieve $\sim$ 1 cpkkd within the energy scale of 0.2–1.2 keVee. Therefore, a lower background level will be required for applications

This work was supported by the National Key Research and Development Program of China (No. 2017YFA0402203), the National Natural Science Foundation of China (No. 11975162), and the Fundamental Research Funds for Central Universities (No. 20822041C4030).

✉ Hao-Yang Xing
xhy@scu.edu.cn

✉ Shu-Kui Liu
liusk@scu.edu.cn

[1] College of Physics, Sichuan University, Chengdu 610064, China

[2] School of Physics, Nankai University, Tianjin 30071, China

[3] Institute of Nuclear Science and Technology, Sichuan University, Chengdu 610065, China

[4] Department of Engineering Physics, Tsinghua University, Beijing 100084, China

used in future ton-scale germanium-based rare event search experiments.

CDEX [8, 11], CDMSLite [10], SuperCDMS [12], and EDELWEISS [9] experiments have been aimed at the direct search of low-mass WIMPs utilizing high-purity germanium (HPGe) detectors. GERDA [13] and Majorana [14] are experiments using enriched ^{76}Ge to detect [15]. The above-mentioned experiments require an ultra-low background. The above studies have shown that the cosmogenic radionuclides inside germanium are among the most important radioactive backgrounds applied in such ultra-low background experiments. Furthermore, because HPGe crystals are exposed directly to cosmic rays, the largest contribution of cosmogenic activity is expected to be during transport, manufacturing, and storage. Therefore, methods to effectively suppress the cosmogenic activation background level in germanium have been an important aspect of these experiments.

To reduce the production rates of long-lived cosmogenic radionuclides, as the most basic and effective method for decreasing the cosmogenic activation, it is necessary to select an appropriate shielding structure and materials in the transport and storage of germanium crystals [14]. However, it is costly and time-consuming to carry out this type of experimental research. Thus, a reliable simulation and calculation are needed for the background of nascent nuclides inside HPGe crystals. Using this method, it is believed that the cosmic background can be effectively calculated and that a reliable estimate can be provided for future ton-scale experiments.

Aguayo et al. [14, 16] provided practical guidance in the choice of shielding materials for cosmic ray particles. Their research showed that an understanding of cosmic ray propagation and attenuation in matter is crucial for an effective shield design. In the selection of a shielding material, both the density and the attenuation length of the cosmic rays are extremely important. In addition, neutrons contribute more than 95% of the cosmogenic nuclear active component (N-component) [17] at sea level. Thus, many studies have been devoted to the attenuation of neutrons of cosmic rays in certain substances, such as water, concrete, and lead [18–20].

Hung et al. [21] measured and simulated a cosmic ray-induced background of HPGe. Through this study, the contribution of environmental radiation to the production rate of radionuclides in HPGe was shown to be less than 0.05%. Therefore, this study mainly considers the effect of cosmic rays on cosmogenic radionuclides. To correctly identify and subtract the background, we analyzed the shielding ability of six materials, i.e., iron, copper, lead, liquid nitrogen, polyethylene, and concrete, to shield cosmic ray particles at different thicknesses using Geant4 and Cosmic-ray Shower Library (CRY) [22] simulations. Furthermore, we optimized the thickness, minimized the overall background count, and provided a better shielding scheme for the transport and storage of HPGe crystals. At the same time, the production rates of the long-lived radionuclides of high-purity germanium crystals under a shielding scheme were obtained, and a quantitative evaluation of the radionuclides was conducted. We expect the simulation results to help reduce the background levels, which is critical for ultra-low background requirements of next-generation ton-scale experiments on HPGe crystals.

2 Methods

2.1 Production mechanisms

At the Earth's surface, when high-energy cosmic rays bombard HPGe crystals, they collide with germanium atoms through elastic scattering, inelastic scattering, and other processes, thereby producing a series of radioactive unstable nuclei inside the crystals. These radionuclides will decay according to their respective half-lives, accompanied by the release of gamma rays, electrons, and other particles, and form the cosmogenic background. The production of radionuclides is an extremely complex process typically involving a wide energy range of 1 MeV to 100 GeV. If R_i is considered the production rate of a radioactive isotope i, it can be expressed as follows:

$$R_i = \sum_j N_i \int \Phi_k(E)\sigma_{kij}\mathrm{d}E, \tag{1}$$

where N_j is the number of stable target nuclear isotopes j, σ_{kij} is the production cross section of radioactive isotope j produced by cosmic ray particle k on target isotope j, and Φ_k is the flux of cosmic ray particle k.

After high-energy cosmic ray bombardment, numerous types of radionuclides are produced, but not all contribute to the cosmogenic background. The major contributors can be found through the decay laws. When HPGe is exposed to cosmic rays, radionuclide decay occurs. The rate of nuclide production can be expressed as follows:

$$P = \frac{\mathrm{d}N}{\mathrm{d}t} + \lambda N, \tag{2}$$

where P is the rate of nuclide production, N is the number of individual nuclides at time t, and λ is a decay constant.

Here, N is given as follows:

$$N = \frac{P}{\lambda}\left(1 - e^{-\lambda t}\right). \tag{3}$$

Clearly, when t approaches infinity, i.e., the exposure time of germanium is sufficiently long, and the number of nuclides produced and the decay become balanced such

that the radionuclides no longer increase in number. This process requires a half-life of 4.3 to reach 95% of the saturation value and a half-life of 6.6 to decay to 1%. Therefore, short-lived nuclei can be eliminated simply by placing the detectors in a deep underground site for a sufficiently long time before experimental data acquisition. Only long-lived nuclei need to be focused on in this study.

2.2 Simulation tools: Geant4 and CRY

The production of radionuclides is a compound process that involves a wide energy range of particles in cosmic ray showers and different types of interactions within the composite shielding materials [23]. In this study, Geant4 was used to simulate the interactions between cosmic rays and the target material. CRY [22] provides information regarding the energy spectrum and flux of the cosmic rays. Geant4 is a toolkit for both a full and fast Monte Carlo simulation of detectors in high-energy physics. The Geant4 package (V10.5p01 + Shielding physics list) was used in this study. CRY software is based on MC calculations used to predict cosmic ray distributions when data are unavailable. This library can generate cosmic ray particles including neutrons, protons, muons, gammas, electrons, and positrons [22] at different altitudes (sea level, 2100 m, and 11,300 m). In this study, we concentrate on the first four particles. The energy, direction, and position sampled from CRY are inputs for the Geant4 simulation program. Taking Chengdu and Beijing as examples, the spectrum information of the cosmic neutrons, protons, muons, and gamma particles can be obtained. Table 1 lists the cosmic ray fluxes calculated by CRY at sea level and at a height of 11,300 m in these cities in 2018.

Clearly, the impact of the altitude and latitude on the cosmic ray flux is extremely large, and thus, the choice of a storage and transport method is crucial. This study takes land transport as an example. Figure 1 shows the spectra of neutrons, protons, muons, and gamma particles at sea level in Chengdu.

Table 1 Cosmic ray fluxes (m-2 s-1) at sea level and at a 11,300 m height in Chengdu and Beijing in 2018

Particles	Beijing (N40°)		Chengdu (N31°)	
	0 m	11,300 m	0 m	11,300 m
Gamma	168.22	22,579.30	163.53	18,017.86
Muon	119.72	754.58	117.65	614.77
Neutron	22.00	9,568.07	18.09	6,248.92
Proton	1.657	706.79	1.45	464.49

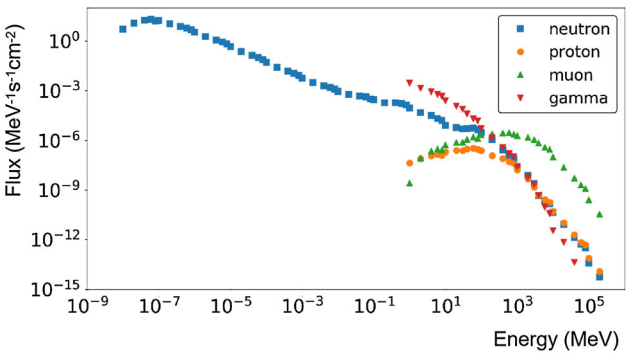

Fig. 1 (Color online) Spectra of cosmic ray neutrons, protons, muons, and gamma particles at sea level in Chengdu

2.3 Simulation details

We simulated two detector geometries in this study. One is a 1 kg cylindrical HPGe crystal with a diameter of 62 mm and a height of 62 mm. The crystal was constructed at the center of an air box and was similar to that used by Ma [23].

The other is a cylindrical HPGe crystal with an outer shielding container, as shown in Fig. 2. The HPGe crystal (Φ 42 cm × 27 cm) was the same size as that used in the GERDA experiment [17]. However, note that the geometry of the crystals has no impact on the production rates of the cosmogenic isotopes because the simulated productivity will be given normalized treatment. For convenient transport, we used a 40-foot container truck. The exterior dimensions of the container are 12.192 m × 2.438 m × 2.591 m, and the interior dimensions are 12.032 m × 2.352 m × 2.385 m. In addition, there is another shielding structure in the container truck. From outside to inside, the initial shielding structure consists of 30-cm-thick polyethylene (with 100-cm-thick polyethylene on top of the crystal), 30-cm-thick iron, 10-cm-thick lead, and a 12-cm-thick copper layer. A schematic diagram of the shielding system is shown in Fig. 2.

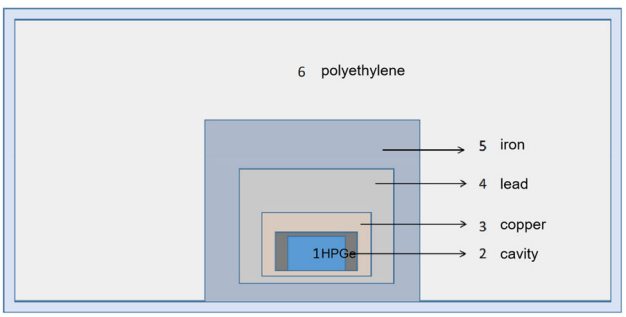

Fig. 2 (Color online) Shielding structure for transport of germanium crystal on the surface: 1, HPGe detector; 2, cavity; 3, oxygen-free copper; 4, lead; 5, iron; and 6, polyethylene

The total mass of the shielding container is 27,873 kg, and the weights of the truck, Fe, PE, Pb, and Cu 40-ft container are 3400, 6448, 13,459, 3079, and 1487 kg, respectively. The deadweight is under 28 t, and the capacity is 67.5 m^3.

The position of each incident particle is randomly extracted from the plane above the detector, the momentum information is randomly extracted from CRY, the energy information is randomly extracted from the CRY-provided energy spectrum, and all secondary particles generated in the detectors are collected and counted.

3 Results and discussion

3.1 Shielding effect of different materials

The shielding effects of iron, lead, copper, liquid nitrogen, polyethylene, and concrete are shown in Fig. 3. Figure 3a–c shows that lead, iron, and copper have a better effect on stopping the primary protons and gamma rays. In addition, materials such as polyethylene and concrete are better choices for neutron shielding. According to previous studies [16, 17], iron has been proved to be an optimal material owing to its lower production rate of secondary neutrons. However, our simulation shows that copper and lead are also appropriate materials, having a lower production rate than iron with a neutron energy of above 10 MeV. By contrast, neutrons at below 10 MeV cannot produce radionuclides in germanium owing to a restriction of the reaction energy threshold, as mentioned in the TENDL data library. Apart from the high-energy secondary neutrons, the primary radionuclides produced in the shielding material also cannot be ignored. The radioactivity of high-purity oxygen-free copper is as low as mBq/Kg order of magnitude. Therefore, considering the cost and weight of the shielding during transport, lead, iron, copper, and polyethylene should be selected as key materials for shielding structures used in the transport of HPGe. Based on the fluxes generated by different cosmic rays from different shielding materials, we analyzed the placement and thickness of the shielding materials. The optimal thickness of each shielding material was obtained by fitting the mass thickness function.

The results of different shielding structures are shown in Fig. 3. As indicated in Fig. 4, the particle count rate decreases from the outside to inside by the shielding. Furthermore, the numbers of protons and gamma particles decrease significantly when passing through the materials, illustrating that these particles are easy to shield. Therefore, the main cosmic ray sources are muons and neutrons. In particular, during the transportation process, a way to effectively shield the neutrons needs to be an area of focus. The simulations show that high-energy neutrons can reduce the amount of energy in polyethylene. Thus, polyethylene is necessary for the effective shielding of neutrons. As shown in Fig. 3, the total neutron count rate decreases by approximately one order of magnitude after being shielded. This demonstrates that the selection order of the shielding materials is reasonable. The proposed composite structures have a meaningful impact on stopping any cosmic rays.

However, the results in Fig. 4 indicate that the shielding of muons is relatively weaker. Therefore, to effectively shield cosmogenic muons, additional structures are needed.

3.2 Cosmogenic production rates of germanium

The cosmogenic production in both detectors described in Sect. 2.3 was simulated using Geant4 and CRY. For the given input energy spectrum of the muons, neutrons, gamma particles, and protons on the Earth's surface, the production rates of several cosmogenic isotopes in natural germanium are calculated. Considering the total production rates, half-life, and energy region of interest, isotopes ^{68}Ge, ^{68} Ga, ^{65}Zn, ^{60}Co, ^{55}Fe, and ^{3}H are the important concern for germanium-based detection experiments [24]. The simulated production rates of cosmogenic isotopes for natural germanium at sea level in Chengdu are listed in Table 2. From Table 2, neutrons contribute to approximately 90% of the production rates of cosmogenic activation. This result is consistent with that of previous studies [23, 24].

As shown in Table 2, the shielding structure significantly reduces the production rates of cosmogenic isotopes from cosmic neutrons, gamma particles, and protons, and the suppression factors are 10 (^{3}H) to 97 (^{55}Fe) for natural germanium. These results demonstrate that a shielding container is necessary when transporting germanium detectors on the Earth's surface.

3.3 Comparison between this study and previous estimates and measurements

Table 3 summarizes the available studies on the calculated and experimental production rates for several isotopes in natural germanium and shows a comparison between our approach and the results of previous production calculations and experiments. As shown in Table 3, the cosmogenic production rates for ^{68}Ge, ^{68} Ga, ^{65}Zn, ^{60}Co, ^{55}Fe, and ^{3}H in natural germanium vary significantly among different model estimates. Such large variations in the production rates are mainly due to the following two reasons:

1. The difference in estimated rates is mainly due to the use of different simulation software and cross-sectional

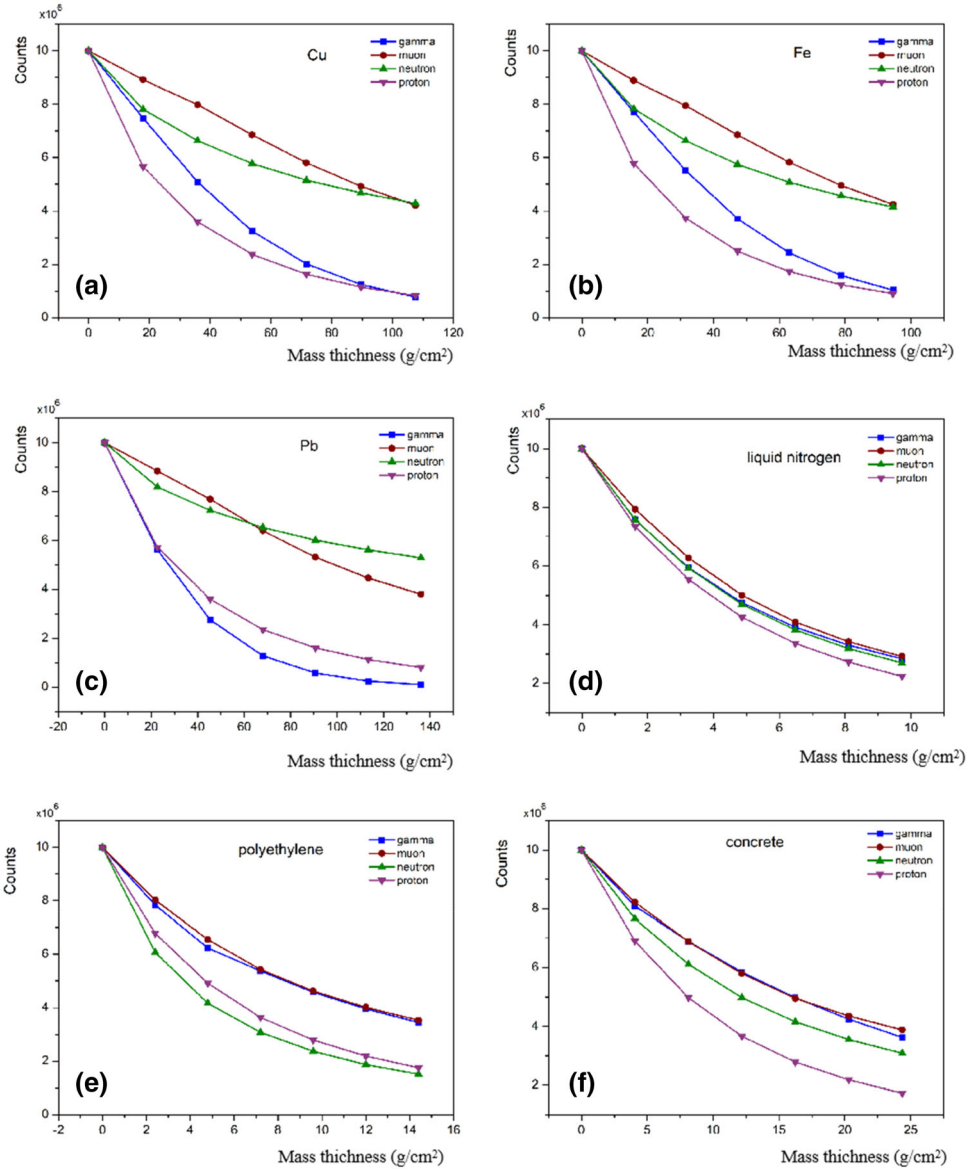

Fig. 3 (Color online) Effect of cosmic rays when using different materials. The abscissa indicates the mass thickness of the material, and the coordinates show the number of outgoing cosmic rays. For all materials applied, the number of primary particles in this simulation is 10^7

libraries. Simulation software can be roughly divided into two categories. One is software calculations based on empirical formulas of isotopic generation cross sections, such as YIELDX [25] and ACTIVIA [26]. The other is software applying a Monte Carlo method to simulate the interactions between incident particles and the target nucleus, such as TALYA [7] and Geant4 [16, 23, 27]. Geant4 is more suitable for simulating the generation of cosmic rays owing to its wide energy range and comprehensive particle cross-sectional data. In addition, when we use the same simulation tool, large differences will occur owing to the different versions applied, e.g., Geant4 versions 3.21 [28], 9.5.02 [24], and 4.10.02 [23]. In addition, the production rates of the cosmogenic isotopes vary significantly among the different Geant4 versions, ranging from a factor of ~ 2 (^{3}H, ^{55}Fe, and ^{65}Zn) to ~ 3 (^{60}Co and ^{68}Ge) for germanium.

2. The second reason is that they input different neutron spectra of cosmic ray. Numerous estimates [17, 19, 29] have come from calculations using historical cosmic ray neutron spectra [30], which are less precise than modern estimates. In addition, calculated or experimentally determined production rates of radioisotopes by cosmogenic activation in natural germanium have been published. Only EDELWEISS [31] and SuperCDMS [32] have published measurements of the production rate of tritium in natural germanium.

As shown in Table 3, our results agree quite well with previous available measurements [23]. The differences among these calculations are mainly due to the use of a

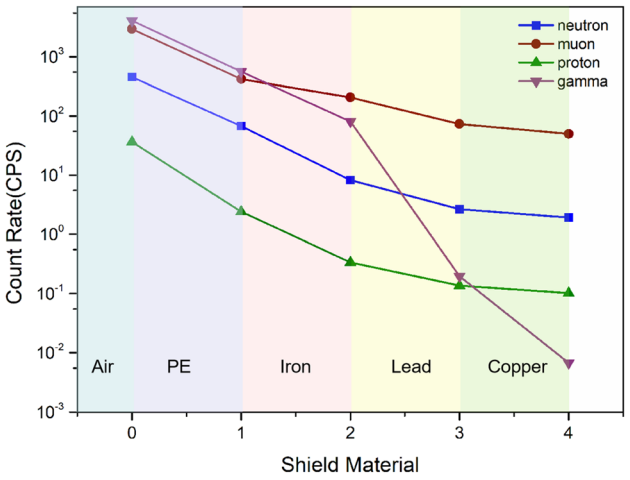

Fig. 4 (Color online) Count rates (cps) of particles produced by different components of cosmic rays. The numbers on the horizontal axis denote the following: 1, polyethylene; 2, iron; 3, lead; and 4, copper

cosmic ray flux in different places and the use of different versions of the simulation tools.

As shown in Table 4, it is worth mentioning that our shield container achieves a higher reduction in the production rates of cosmogenic isotopes in germanium. Compared with iron shields, our shield exhibits an improvement in suppression by one order of magnitude between these isotopes for natural germanium. They are mostly produced by an inelastic scattering of neutrons. The reduction of ^{60}Co and ^{68}Ge has an actual meaning in $0\nu\beta\beta$ experiments, and ^{3}H may have a significant impact on the sensitivity of germanium-based detectors for future ton-scale experiments in the direct detection of low-mass dark matter particles. The end point energy of ^{3}H beta decay is only $\sim$18.6 keV. This implies that the entire energy spectrum of ^{3}H can contribute to the background of a low-energy region for low-mass dark matter detection [24]. The lifetimes of ^{3}H, ^{60}Co, and ^{68}Ge are particularly long, which makes it difficult to eliminate these radioactive isotopes by simply placing the detectors deep underground, and thus,

Table 2 Production rates of cosmogenic isotopes in natural germanium at sea level as estimated using Geant4 with and without a shield in Chengdu

Isotope	$T_{1/2}$	Neutron		Proton		Muon		Total	
		No shield	Shield	No shield	Shield	No shield	Shield	No shield	Shield
^{68}Ge	270 d	58.78	2.67	4.45	0.48	0.38	2.93	63.61	6.08
^{65}Zn	2.7 y	23.38	0.63	3.01	0.18	1.28	1.33	27.67	2.14
^{60}Co	5.3 y	0.69	0.02	0.18	0	0.03	0.05	0.9	0.07
^{55}Fe	244.3 d	2.17	0.02	0.72	0.01	0.04	0	2.93	0.03
^{3}H	12.3 y	15.66	0.18	5.62	0.14	0.28	0.13	21.56	0.45

Table 3 Production rates of cosmogenic isotopes estimated in this study for natural germanium without shielding at sea level. The production rates at sea level in Beijing use (a) Geant4 version 4.10.03 and (b) Geant4 version 4.10.05. In addition, the production rates in (a) Beijing and (c) Chengdu are compared with previous published calculated and experimental results

References	Method	Production rate (Kg^{-1} day^{-1})				
		^{3}H	^{55}Fe	^{60}Co	^{65}Zn	^{68}Ge
Avignone [29]	Calc	210	–	–	34.4	29.6
Klapdor [28]	Calc	–	8.4	6.6	79	58.4
Barabanov [17]	Calc	–	-	2.86	–	81.6
Back [26]	Calc	–	3.4	2.8	29	45.8
Mei [7]	Calc	27.7	8.6	2.0	37.1	41.3
Cebrian [25]	Calc	–	6	3.9	63	60
EDELWEISS [27]	Calc	43.5	4	–	65.8	45
Wei [24]	Calc	47.37	7.91	2.87	75.93	182.8
Ma [23]	Calc	23.68	4.15	1.45	40.47	83.05
SuperCDMS [32]	Calc	95	5.6		51	49
This work	Calc.(a)	24.43	4.65	1.44	39.85	82.58
	Calc.(b)	25.62	3.45	1.09	35.03	80.71
	Calc.(c)	21.56	2.93	0.90	27.67	63.61
EDELWEISS [27]	Exp	82 ± 21	4.6 ± 0.7	-	106 ± 13	> 71
SuperCDMS [32]	Exp	74 ± 9	1.5 ± 0.7	-	17 ± 5	30 ± 18

Table 4 Production rates (kg^{-1} day^{-1}) of cosmogenic isotopes in germanium at sea level as estimated using Geant4 with a shield container. In previous iron shield calculations [24], the iron shield structure is the same as that used in GERDA

Isotope	$T_{1/2}$	Neutron		Proton		Muon		Total	
		Iron shield [24]	Shield (our)	Iron shield [24]	Shield (our)	Iron shield [24]	Shield (our)	Iron shield [24]	Shield (our)
^{68}Ge	270 d	46.05	2.67	0.53	0.48	3.86	2.93	50.44	6.08
^{65}Zn	244.3 d	16.87	0.63	0.24	0.18	0.68	1.33	17.79	2.14
^{60}Co	5.3 y	0.57	0.02	0.009	0	0.091	0.05	0.67	0.07
^{55}Fe	2.7 y	0.94	0.02	0.02	0.01	0.061	0	1.02	0.03
^{3}H	12.3 y	8.59	0.18	0.19	0.14	0.88	0.13	9.66	0.45

the only way to reduce these backgrounds is to limit the exposure of the crystal when it is grown and transported [27]. Therefore, reducing the production rates of ^{3}H, ^{60}Co, and ^{68}Ge using a shield is extremely meaningful for rare event search experiments.

4 Conclusion

In this study, we investigated the effects of the production of cosmogenic radioactivity in the storage and transport of germanium when applying a cosmic ray shield based on the MC simulation programs: Geant4 and CRY. Based on the analysis of several shielding materials and the structure of the shield itself, we provided a better shielding design for the transport and storage of high-purity germanium. At the same time, a relatively complete calculation of the numbers of radionuclides inside HPGe was determined. The production rates of cosmogenic radionuclides are reduced by approximately one order of magnitude by adding an optimized shielding structure. The validity of the simulation was confirmed through a comparison with a previous study. The proposed method can be applied to quantitatively evaluate the number of terrestrial radionuclides in other materials by adjusting only certain conditions, such as the types of cosmic rays and materials. According to this simulation, if lower overall background count rates can be effectively achieved, it will help the suppression of background events during rare event search experiments.

References

1. S.M. Bilenky, Neutrinoless double beta-decay. Phys. Part. Nucl. **41**, 690–715 (2010). https://doi.org/10.1134/S1063779610050035
2. K. Zuber, Neutrinoless double beta decay experiments. Acta Physica Polonica. **37**, 1905–1921 (2006). https://doi.org/10.1088/1748-0221/1/07/P07002
3. D.O. Stefano, M. Simone, V. Matteo et al., Neutrinoless double beta decay: 2015 review. Adv. High Energy Phys. **2016**, 2162659 (2016). https://doi.org/10.1155/2016/2162659
4. G. Bertone, The moment of truth for WIMP dark matter. Nature **468**, 389–393 (2010). https://doi.org/10.1038/nature09509
5. J.D. Lewin, P.F. Smith, Review of mathematics, numerical factors, and corrections for dark matter experiments based on elastic nuclear recoil. Astropart. Phys. **6**, 87–112 (1996). https://doi.org/10.1016/S0927-6505(96)00047-3
6. J. Schechter, J. Valle, Neutrinoless double- decay in SU(2)×U(1) theories. Phys. Rev. D. **25**, 2951–2954 (1982). https://doi.org/10.1103/PhysRevD.25.2951
7. D.M. Mei, Z.B. Yin, S.R. Elliott, Cosmogenic production as a background in searching for rare physics processes. Astropart. Phys. **31**, 417–420 (2009). https://doi.org/10.1016/j.astropartphys.2009.04.004
8. K. Kang, J. Cheng, J. Li et al., Introduction to the CDEX experiment. Front. Phys.-Beijing. **8**, 412–437 (2013). https://doi.org/10.1007/s11467-013-0349-1
9. L. Hehn, E. Armengaud, Q. Arnaud et al., Improved EDELWEISS-III sensitivity for low-mass WIMPs using a profile likelihood approach. Eur. Phys. J. C. **76**, 548 (2016). https://doi.org/10.1140/epjc/s10052-016-4388-y
10. R. Agnese, A.J. Anderson, T. Aralis et al., Low-mass dark matter search with CDMSlite. PHYS REV D. **97**, 022002 (2018). https://doi.org/10.1103/PhysRevD.97.022002
11. L. Wang, Q. Yue, K. Kang et al., First results on Ge-76 neutrinoless double beta decay from CDEX-1 experiment. Sci. China Phys. Mech. **60**, 071011 (2017). https://doi.org/10.1007/s11433-017-9038-4
12. R.W. Schnee, D.S. Akerib, M.J. Attisha, et al., The SuperCDMS experiment. In: Klapdor-Kleingrothaus H.V., Arnowitt R. (eds) Dark Matter in Astro- and Particle Physics. Springer, Berlin, pp. 259–268. https://doi.org/10.1007/3-540-26373-X_20
13. L. Pandola, C. Tomei, GERDA, a GERmanium Detector Array for the search for neutrinoless betabeta decay in ^{76}Ge. AIP Conf. Proc. **842**, 843 (2006). https://doi.org/10.1063/1.2220398
14. N. Abgrall, E. Aguayo, F.T.I. Avignone et al., The MAJORANA DEMONSTRATOR Neutrinoless Double-Beta Decay Experiment. Adv. High Energy Phys. (2014). https://doi.org/10.1155/2014/365432
15. H. Jiang, L.P. Jia, Q. Yue et al., Limits on light weakly interacting massive particles from the first 102.8 kg × day data of the CDEX-10 experiment. Phys. Rev. Lett. **120**, 241301 (2018). https://doi.org/10.1103/PhysRevLett.120.241301
16. E. Aguayo Navarrete, R.T. Kouzes, A.S. Ankney, et al., Cosmic ray interactions in shielding materials. In: Pacific Northwest

National Laboratory Report (2011). https://doi.org/10.2172/1025678
17. I. Barabanov, S. Belogurov, L. Bezrukov et al., Cosmogenic activation of germanium and its reduction for low background experiments. Nucl. Instrum. Meth. B. **251**, 115–120 (2006). https://doi.org/10.1016/j.nimb.2006.05.011
18. G. Cocconi, V.C. Tongiorgi, Intensity and Lateral Distribution of the N-Component in the Extensive Showers of the Cosmic Radiation. Phys. Rev. **79**, 730–732 (1950). https://doi.org/10.1103/PhysRev.79.730
19. J.F. Ziegler, G.R. Srinivasan, Terrestrial cosmic rays and soft errors. IBM J. Res. Dev. **40**, 19–39 (1996). https://doi.org/10.1147/rd.401.0019
20. J. Tinlot, B. Gregory, Absorption of Penetrating Shower Primaries. Phys. Rev. **75**, 519–520 (1949). https://doi.org/10.1103/physrev.75.519
21. N.Q. Hung, V.H. Hai, M. Nomachi, Investigation of cosmic-ray induced background of Germanium gamma spectrometer using GEANT4 simulation. Appl. Radiat. Isotopes. **121**, 87–90 (2017). https://doi.org/10.1016/j.apradiso.2016.12.047
22. P. Papini, C. Grimani, S.A. Stephens, An estimate of the secondary-proton spectrum at small atmospheric depths. IL Nuovo Cimento C. **19**, 367–387 (1996). https://doi.org/10.1007/BF02509295
23. J. Ma, Q. Yue, S. Lin et al., Study on cosmogenic activation in germanium detectors for future tonne-scale CDEX experiment. Sci. China Phys. Mech. **62**, 11011 (2019). https://doi.org/10.1007/s11433-018-9215-0
24. W.Z. Wei, D.M. Mei, C. Zhang, Cosmogenic activation of germanium used for tonne-scale rare event search experiments. Astropart. Phys. **96**, 24–31 (2017). https://doi.org/10.1016/j.astropartphys.2017.10.007
25. S. Cebrián, J. Amaré, B. Beltrán et al., Cosmogenic activation in germanium double beta decay experiments. J. Phys. Conf. **39**, 344–346 (2006). https://doi.org/10.1088/1742-6596/39/1/089
26. J.J. Back, Y.A. Ramachers, ACTIVIA: Calculation of isotope production cross-sections and yields. Nucl. Instrum. Meth. A. **586**, 286–294 (2008). https://doi.org/10.1016/j.nima.2007.12.008
27. E. Armengaud, Q. Arnaud, C. Augier et al., Performance of the EDELWEISS-III experiment for direct dark matter searches. J. Instrum. (2017). https://doi.org/10.1088/1748-0221/12/08/P08010
28. H.V. Klapdor-Kleingrothaus, L. Baudis, A. Dietz et al., GENIUS-TF: a test facility for the GENIUS project. Nucl. Instrum. Meth. A. **481**, 149–159 (2002). https://doi.org/10.1016/s0168-9002(01)01258-x
29. F.T. Avignone, R.L. Brodzinski, J.I. Collar et al., Theoretical and experimental investigation of cosmogenic radioisotope production in germanium. Nucl. Phys. B. **28**, 280–285 (1992). https://doi.org/10.1016/0920-5632(92)90184-T
30. W.N. Hess, H.W. Patterson, R. Wallace et al., Cosmic-ray neutron energy spectrum. Phys Rev. **116**, 445–457 (1959). https://doi.org/10.1103/PhysRev.116.445
31. E. Armengaud, Q. Arnaud, C. Augier et al., Measurement of the cosmogenic activation of germanium detectors in EDELWEISS-III. Dark Matter Astro Particle Phys. **91**, 51–64 (2017). https://doi.org/10.1016/j.astropartphys.2017.03.006
32. R. Agnese, T. Aralis, T. Aramaki et al., Production rate measurement of Tritium and other cosmogenic isotopes in Germanium with CDMSlite. Astropart. Phys. **104**, 1–12 (2019). https://doi.org/10.1016/j.astropartphys.2018.08.006